JACS
JOURNAL OF THE AMERICAN CHEMICAL SOCIETY

Article

pubs.acs.org/JACS

Coupling and Decoupling of Rotational and Translational Diffusion of Proteins under Crowding Conditions

Matthias Roos,[†,§] Maria Ott,[†,§] Marius Hofmann,[‡] Susanne Link,[†] Ernst Rössler,[‡] Jochen Balbach,[†] Alexey Krushelnitsky,[*,†] and Kay Saalwächter[*,†]

[†]Institut für Physik, Martin-Luther-Universität Halle-Wittenberg, 06099 Halle (Saale), Germany

[‡]Experimentalphysik II, Universität Bayreuth, 95440 Bayreuth, Germany

Supporting Information

ABSTRACT: Molecular motion of biopolymers *in vivo* is known to be strongly influenced by the high concentration of organic matter inside cells, usually referred to as crowding conditions. To elucidate the effect of intermolecular interactions on Brownian motion of proteins, we performed ^{1}H pulsed-field gradient NMR and fluorescence correlation spectroscopy (FCS) experiments combined with small-angle X-ray scattering (SAXS) and viscosity measurements for three proteins, αB-crystalline (αBc), bovine serum albumin, and hen egg-white lysozyme (HEWL) in aqueous solution. Our results demonstrate that long-time translational diffusion quantitatively follows the expected increase of macro-viscosity upon increasing the protein concentration in all cases, while rotational diffusion as assessed by polarized FCS and previous multi-frequency ^{1}H NMR relaxometry experiments reveals protein-specific behavior spanning the full range between the limiting cases of full decoupling from (αBc) and full coupling to (HEWL) the macro-viscosity. SAXS was used to study the interactions between the proteins in solution, whereby it is shown that the three cases cover the range between a weakly interacting hard-sphere system (αBc) and screened Coulomb repulsion combined with short-range attraction (HEWL). Our results, as well as insights from the recent literature, suggest that the unusual rotational−translational coupling may be due to anisotropic interactions originating from hydrodynamic shape effects combined with high charge and possibly a patchy charge distribution.

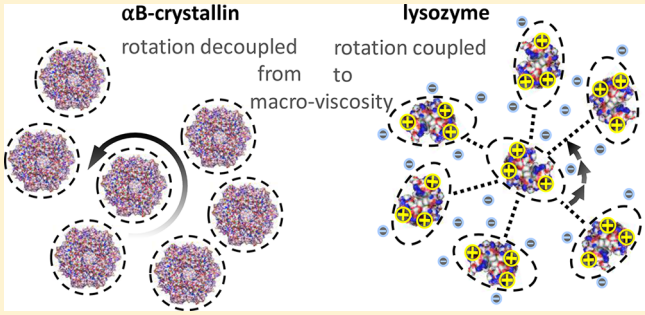

INTRODUCTION

Inside cells, macromolecules occupy 20−40% of the cytoplasmic volume,[1,2] providing an environment in which the mean distance between neighboring particles is similar to their size. Highly concentrated solutions of proteins and other organic molecules mimicking the cell interior are usually referred to as crowded environment.[3−5] Crowding affects many aspects of cellular function and organization,[6,7] including biochemical reactions, enhanced protein refolding rates, and the stabilization or destabilization of the compact folded states.[8−11] In particular, crowding sensitively affects *in vivo* molecular motion,[12] where protein Brownian dynamics is rather complex due to the usually non-spherical shape of the globule and its complex non-symmetric electrostatic interactions.

The Brownian dynamics of concentrated particle suspensions can be quantitatively described by mean-field models that depend only on the overall volume fraction ϕ of the dispersed particles. This leads to the generalized Stokes−Einstein (GSE) and generalized Stokes−Einstein−Debye (GSED) relationships for the long-time translational diffusion coefficient D^L and the rotational correlation time τ_r, respectively:

$$D^L(\phi) = \frac{k_B T}{6\pi\eta(\phi)R_H} \quad (1)$$

$$\tau_r(\phi) = \frac{4\pi\eta(\phi){R_H}^3}{3k_B T} \quad (2)$$

where R_H and k_BT denote the hydrodynamic radius and the thermal energy, respectively. For the generalized forms, the solvent viscosity η_0 is merely replaced by the macroscopic dispersion viscosity $\eta(\phi)$; for a critical discussion see ref 13. Such a treatment implies that a macromolecular solute is surrounded by an effective, continuous medium—a situation that is, at first glance, violated under crowding conditions. However, it is well established that the GSE relation for translational diffusion, eq 1, holds for concentrated hard-sphere (HS)[14−16] and even soft colloid systems,[17] but does not necessarily hold for charge-stabilized colloids.[13,15] Crowded proteins represent, in general, a case in-between these limiting situations.

Received: June 27, 2016
Published: July 19, 2016

DOI: 10.1021/jacs.6b06615
J. Am. Chem. Soc. 2016, 138, 10365−10372

The validity of the GSED relationship, eq 2, has not yet unambiguously been assessed for proteins. In the presence of neighboring particles, rotational diffusion depends on the particle shape[18] and on intermolecular electrostatic interactions[19] that are, concerning proteins, usually of rather complex nature due to a non-symmetric charge distribution within the protein. Despite the high interest in crowding effects for understanding *in vivo* behavior of proteins, the effect on Brownian dynamics remains little studied and controversial. Notably, recent combined studies of translational and rotational diffusion of proteins contradict each other with regards to the effect of crowding: it remains unclear whether rotational diffusion becomes less retarded[20] than translational diffusion of the protein, or *vice versa*.[21] Thus, assessing the potential applicability of both the GSE and GSED relationships is of high relevance to ultimately link microscopic observables with biological function.

Recently we have undertaken a detailed nuclear magnetic resonance (NMR) study of the Brownian dynamics of the eye-lens protein αB-crystallin (αBc) over a wide range of concentrations.[22] We found a pronounced decoupling between translational and rotational diffusion: while the slow-down of translational diffusion upon increasing the protein concentration perfectly matched the increase in macro-viscosity, rotational diffusion was almost unaffected. This effect can be explained in terms of a "caging" of the probed molecule by surrounding ones,[23−25] and is generally linked to the phenomenon of the colloidal glass transition.[26−28] Indeed, a HS-like glass transition in eye-lens α-crystallin solutions was shown recently.[29] Notably, the stable αBc assembly has a rather symmetric, quasi-spherical shape[30] as it consists of several symmetrically arranged monomers,[30] such that it resembles an almost perfect hard-sphere particle,[31] while other proteins may not. Thus, the behavior of αBc can hardly be taken as universal.

In the present work, we extend our studies by two other proteins, bovine serum albumin (BSA) and hen egg white lysozyme (HEWL). We show that the coupling or decoupling of rotational and long-time translational diffusion under crowding conditions is protein-specific and appears to be related to the specific type of interactions between neighboring proteins.

Protein molecular mobility is characterized here by both NMR spectroscopic measurements of translational and rotational[22,32] diffusion and independent measurements of the same quantities by polarized fluorescence correlation spectroscopy (FCS). These data are complemented by measurements of the macroscopic viscosity and the intermolecular interactions by capillary rheology and small-angle X-ray scattering (SAXS), respectively. Short-time translational diffusion coefficients from neutron-scattering literature data[33] are also taken into account. The combined results provide a comprehensive picture on the Brownian dynamics of proteins under "self-crowding" conditions.

MATERIALS AND METHODS

Samples. Native α-crystallin is a spherical assembly of two homologous proteins, αA-crystallin (αAc) and αBc, each of a monomer molecular mass of ∼20 kDa. The α-crystallin complex has a molecular mass distribution from 500 to 1000 kDa, with the average mass around 800 kDa. Subunit exchange occurs on the time scale of minutes[34] and is much slower than the time scale of our experiments. Here, we rely on our previous data reporting on pure human αBc in buffer solution. In fact, pure αBc has very similar properties to the mixture of αAc and αBc. For details, also concerning recombinant αBc purification, see ref 22.

HEWL from chicken egg white and fatty acid-free BSA were obtained from Sigma-Aldrich (product numbers 62970 and A7030, respectively) as lyophilized powders and dissolved in D_2O to keep the water NMR signal low. Via lyophilizing and dissolving the protein solution once again in D_2O, residual water proteins were further reduced. No buffer was added to ensure almost unscreened electrostatic interactions. The pD obtained was pD 3.8 for HEWL and pD 7.0 for BSA (isoelectric points of pH 11.35 and pH 4.7, respectively). No significant pD changes (more than 0.1−0.2) were observed upon varying the protein concentration. Under these conditions, HEWL (14.4 kDa) is a strongly charged monomeric protein[32] soluble up to high concentrations. BSA consists of monomers (66.4 kDa) and about 50% long-time stable oligomers of different sizes.[32,35]

Experiments. Translational diffusion coefficients were determined using a Bruker Avance II spectrometer with a ^{1}H resonance frequency of 400 MHz, using a Diff60 probehead. Pulsed field gradient (PFG) NMR diffusion decays were obtained by use of the stimulated echo technique applying bipolar gradient pulses, and were fitted by

$$A(g) = A(0)\exp(-\gamma^2 g^2 D^L \delta^2(\Delta - \delta/3)) \quad (3)$$

in which $A(g)$ is the (integral) signal intensity in dependence of the gradient strength g, and γ is the ^{1}H gyromagnetic ratio. δ and Δ denote the fixed gradient pulse duration and diffusion time, respectively. Exemplary PFG NMR diffusion decays for αBc, BSA, and HEWL are shown in ref 22 and the Supporting Information (SI1); data for BSA and HEWL were measured within this work. Translational protein diffusion as characterized by PFG NMR relies on diffusion times of a few tens of milliseconds, thus providing translational displacements in the μm range. Hence, PFG NMR probes protein translational diffusion in the long-time limit.

NMR data for rotational diffusion rely on longitudinal relaxation rates (R_1) measured on a field-cycling instrument and/or rotating-frame ($R_{1\rho}$) and transverse (R_2) relaxation rate measurements of the integral ^{1}H signal. The derived rotational correlation times are taken from our previous publications; see refs 22 and 32.

Rotational correlation times τ_r and translational diffusion times τ_D were also determined by polarized FCS with alternating orthogonal, linearly polarized excitation. We used a home-built setup similar to the one described in ref 36; see SI2 for details on the setup, sample preparation, and data processing. Polarized FCS probes rotations of the transition dipole moment and relies on the use of linearly polarized excitation of protein-bound dyes and separate detection of the two orthogonal emission components on a single-molecule basis. The two signals of the fluorescence components that are collinear to the excitation pulses are then cross-correlated, yielding a time correlation function; see Figure 1. Its initial rise (exponential in nature) encodes τ_r, while its long-time decay encodes τ_D, the time needed by the molecule to leave again the detection volume. For the latter, due to the well-known issues with focal volume calibration, we refrained from converting it into absolute values for D^L.

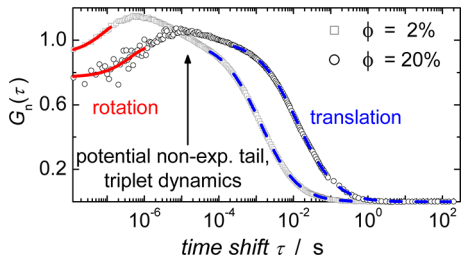

Figure 1. Normalized cross-correlation functions $G_n(\tau)$ from polarized FCS with alternating orthogonal, linearly polarized excitation for BSA at two concentrations, including fits to obtain τ_r (solid red lines) and τ_D (dashed blue lines).

DOI: 10.1021/jacs.6b06615
J. Am. Chem. Soc. 2016, 138, 10365−10372

Steady-shear viscosities were measured at a shear rate of 1000 or 2000 s^{-1} using the microfluid viscometer m-VROC (Rheosense Inc., CA). Upon decreasing the shear rate to 100 s^{-1}, the signal-to-noise ratio decreased, yet no effect on the viscosity measured was found. Despite the rather high shear rates, the measurements still provide the macro-viscosity.

SAXS measurements were performed at 20 °C using an X-ray generator of rotating anode type with Cu target from Rigaku, operated at 2.4 kW, and a 2D gas detector. Generally, the SAXS signal $I(q)$ can be written as a product of the form factor $F(q)$ and the structure factor $S(q)$; $I(q) = F(q)S(q)$. The form factor contains information regarding the 3D shape of the scattering particles and was determined at low concentrations (0.5−2 vol%) and electrostatic screening conditions. The structure factor does not depend on the shape of the particles but contains the inter-particle interactions, and is determined at different protein concentrations of BSA, HEWL, and αBc by $S(q) = I(q)/I_0(q)\cdot c_0/c$. For details, see SI3.

RESULTS

Figure 2 presents the temperature dependence of long-time translational diffusion (a) and viscosity (b). For both cases and all proteins, we observe activation energies (E_A) close to 20 kJ/mol that increase only slightly with concentration, indicating that both quantities are largely governed by the solvent viscosity (water). This important result also indicates that *transient* or crowding-induced binding among the proteins is of little relevance, as such an effect would lead to a significantly increased apparent E_A for translational diffusion.[37] At higher concentration, however, HEWL exhibits non-Arrhenius (Vogel−Fulcher-like) behavior, reflecting increased inter-particle interactions.

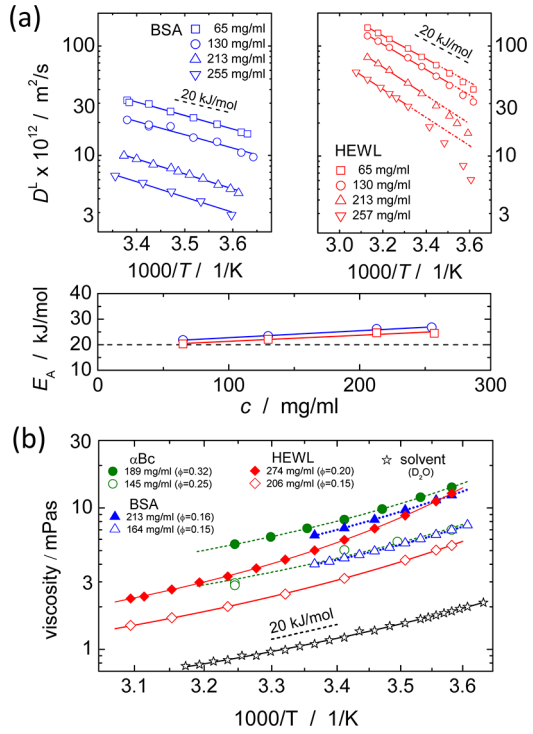

Figure 2. Temperature dependence of long-time translational diffusion (a) and viscosity (b) for HEWL, BSA, and αBc. Black dashed lines indicate the slope corresponding to E_A = 20 kJ/mol. For HEWL translational diffusion, only the high-temperature region was used to estimate E_A as plotted in the lower panel in (a). The αBc viscosity data were already published in ref 22.

The data for rotational diffusion from multi-frequency relaxometry published in our previous publications[22,32] show the same trends in E_A as discussed above for translational diffusion and viscosity. A detailed comparison of all quantities is deferred to the Discussion section. It should just be noted that the molecular tumbling times τ_r, as reported in ref 22 and the Supporting Information of ref 32, are subject to a potentially large systematic error when neglecting the, at higher concentrations, increasingly nonexponential tailed character of the tumbling correlation function (TCF) in the NMR relaxation data analysis. We have so far used an ad-hoc phenomenological approach, representing the unknown complex TCF as a superposition of two exponentials, $C_{2exp}(t)$, with a minority component featuring a much slower decay time constant τ_s and comparably low amplitude a_s. In order to assess the influence of this "slow tail" on the reported rotational correlation time, and to enable a comparison with the value from FCS, we also consider an apparent correlation time defined as the inverse of the initial slope of the fitted apparent TCF:

$$\tau_{r,ini} = \left\langle \frac{dC_{2exp}(t)}{dt} \right\rangle_{t=0}^{-1} = \left[\frac{1 - a_s}{\tau_r} + \frac{a_s}{\tau_s} \right]^{-1} \quad (4)$$

It is important to note that τ_r from FCS, due to the restriction of the exponential fit to the initial time range of the FCS cross-correlation function $G_n(\tau)$, provides the same quantity as given by eq 4.

Figure 3 compares $\tau_{r,ini}$ with τ_r (the apparent primary tumbling time) determined by both NMR and FCS. Despite its large influence on the NMR data analysis, the apparent "slow tail" is thus demonstrated to have a nearly negligible influence on $\tau_{r,ini}$ in the studied concentration range. Additional uncertainty arises from the non-spherical shape of the protein,[38] but as shown in SI4, considering tensorial rotational diffusion has little influence on the fitted absolute value of τ_r and its concentration dependence. In view of the potentially large uncertainties related to a complex and not necessarily multi-exponential overall correlation function,[39,40] the coincidence between NMR and FCS data, as well as the agreement with the values estimated on the basis of R_H from translational diffusion

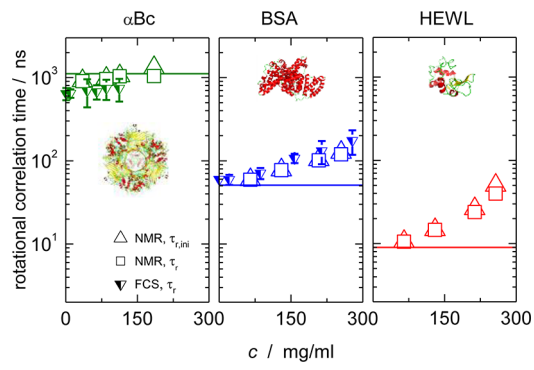

Figure 3. Comparison of tumbling times determined by NMR relaxometry ($\tau_{r,ini}$ and τ_r; the symbol size reflects the experimental uncertainty) and FCS for the three proteins. The solid lines indicate approximate dilute-limit values calculated from eq 2 using R_H calculated from eq 1, using D^L from PFG NMR at the lowest concentrations. Within each diagram a visual presentation of the protein (not to scale) is shown based upon Protein Data Bank structures (PDB IDs 2YGD, 4F5S, and 1LYZ).

DOI: 10.1021/jacs.6b06615
J. Am. Chem. Soc. 2016, 138, 10365−10372

in the most dilute cases, represents a relevant finding. Note that a (possibly non-exponential) long-time tail of the TCF would contribute to the FCS cross-correlation function at intermediate times, but is not reliably detectable due to its low amplitude and additional contributions from triplet dynamics and the onset of translational diffusion (see Figure 1).

The deviation of τ_r from NMR and FCS for αBc can be explained by the polydispersity of this protein, which is taken into account in different ways in NMR and FCS experiments; see SI5. This deviation is relevant mainly for dilute-limit data and does not challenge any conclusions on crowding effects. As to the latter, from the data in the given semi-logarithmic representation, we mainly take that the relative increase of $\tau_{r(,ini)}$ with concentration differs significantly among the samples, as analyzed further below.

In order to characterize and compare directly the nature of the inter-particle interactions, we have measured SAXS data for the three proteins under study, see Figure 4 and SI3. This information is of course subject to the limitation that an isotropic average is obtained. The structure factors exhibit qualitative differences. They suggest that αBc assemblies behave like hard spheres, while BSA and HEWL are dominated by Coulomb interactions. In the latter case, short-range attractive interactions are to be considered as well. Details on the corresponding analyses, and the concentration effects on the structure factors, will be discussed in the next section.

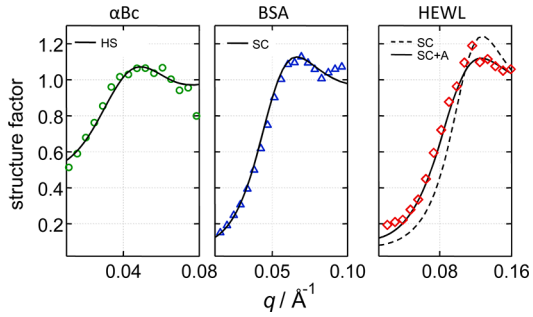

Figure 4. Protein interaction strength as assessed by SAXS structure factors for a volume fraction of ϕ = 10%. The fits to hard-sphere (HS), screened Coulomb (SC), and SC plus short-range attraction (SC+A) models for αBc, BSA, and HEWL, respectively, are discussed in the next section.

DISCUSSION

Long-Time Translational Diffusion Scales with Macroscopic Viscosity. For a direct comparison of the concentration dependence of viscosity and translational and rotational diffusion in one and the same plot, we compare inverse reduced diffusion coefficients $(D^L/D_0^L)^{-1}$, reduced tumbling or translational diffusion times $(\tau_{r/D}/\tau_{r/D,0})$, and normalized viscosities (η/η_0) at 20 °C, all referred to as retardation factor r. In this way, Figure 5 shows r with increasing extent of crowding (see SI6 for absolute values) and presents the central result of this work. Note in particular that the slope of the data is independent of the chosen reference concentration, as the retardation factors are plotted on a semi-logarithmic scale. As seen from Figure 5, for all cases the reduced long-time translational self-diffusion coefficients match the increase of viscosity with concentration, i.e., $D^L(\phi)/D_0^L = \eta_0/\eta(\phi)$. This demonstrates the applicability of the GSE relation, eq 1.

In Figure 5, the steric volume fraction was defined as $\phi = c\vartheta$, where ϑ is the specific volume of the protein (ϑ = 1.7 mL/g,[41] 0.735 mL/g,[33] and 0.702 mL/g[42] for αBc, BSA, and HEWL, respectively). See SI7 for the actual data. The large specific volume for αBc (i.e., low density) results from its high molecular weight combined with the deviation of most "globular" proteins from compact-globule scaling: $V \propto M^{1.2}$ rather than $V \propto M$.[1,22,43]

The applicability of the GSE equation as observed in the present three cases is in full accordance with established colloid-science concepts: during translational diffusion in the long-time limit, the particle's trajectory averages over many different configurations of its local surrounding, which allows for a description of the inhomogeneous environment acting in terms of an effective medium of (zero-shear) viscosity $\eta(\phi)$.[13]

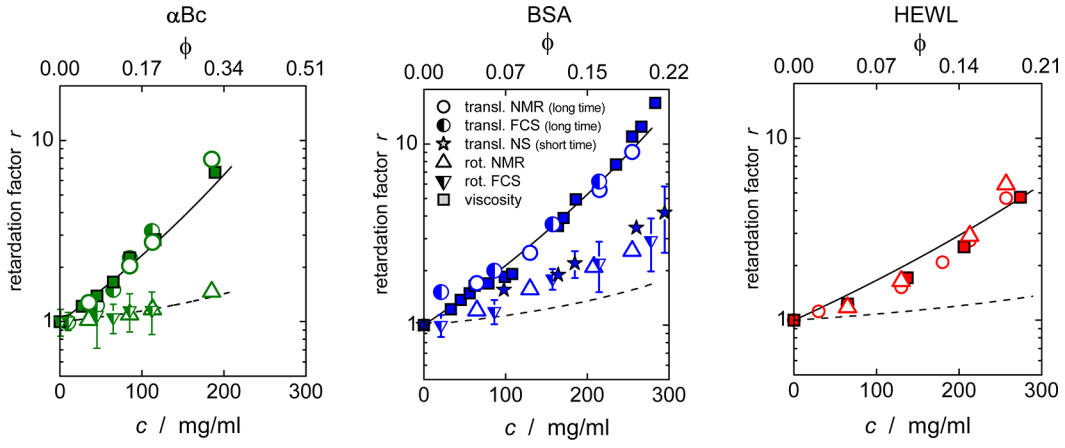

Figure 5. Retardation of long-time translation (circles) and rotation (triangles) as compared to viscosity (squares) in dependence of the protein concentration c. The retardation factors are the respective measured quantities normalized against their low-concentration limits. For NMR, they are normalized to an extrapolated value (see SI6), while for FCS we have experimental results at virtually zero (nM) concentration. If not indicated by error bars, experimental uncertainties are of the order of or smaller than the symbol size. Short-time translational diffusion data observed for BSA by neutron scattering (stars) are reproduced from ref 33. Data of αBc and all NMR rotational diffusion data are taken from our previous publications.[22,32] The solid lines correspond to predictions of long-time translational diffusion, eq 5, and are based upon an effective HS volume fraction, $\phi_{HS} = k\,\phi$ (k = 1, 2.1, and 1.5 for αBc, BSA, and HEWL, respectively). The dashed lines are HS predictions for rotational diffusion, eq 6, using the same rescaling factor k as obtained for translational diffusion.

DOI: 10.1021/jacs.6b06615
J. Am. Chem. Soc. 2016, 138, 10365−10372

In the literature, both accordance[21,44] and mismatch[20,21] between translational diffusion and viscosity were reported. It is important to note that, in studies reporting on a mismatch, tracer and crowding agent were different proteins, or even synthetic polymer crowders (Ficoll, polyethylene glycol) were used. In such studies, translational diffusion measurements solely report on the tracer species, whereas viscosity measurements are strongly dominated by the specific interactions among the crowder molecules due to their much higher volume fraction. For diffusion of the tracer proteins mixed with *other* proteins, transient binding may be important.[37]

Quantitatively, the slow-down of long-time translational diffusion has been addressed via HS models,[45] resulting in

$$\frac{D^{\mathrm{L}}(\phi_{\mathrm{HS}})}{D_0^{\mathrm{L}}} \cong \frac{(1-\phi_{\mathrm{HS}})^3}{1+(3/2)\phi_{\mathrm{HS}}+2{\phi_{\mathrm{HS}}}^2+3{\phi_{\mathrm{HS}}}^3} \quad (5)$$

Proteins are subject to intermolecular interactions beyond the pure HS potential, in particular through electrostatic interactions. However, the size of the protein can be re-adjusted by use of an *effective* HS radius, corresponding to an effective HS volume fraction $\phi_{\mathrm{HS}} = k\,\phi$, $k \geq 1$. Fits to eq 5 shown in Figure 5 correspond to $k = 1$, $k = 2.1$, and $k = 1.5$ for αBc, BSA, and HEWL, respectively. Note that k is the only adjustable parameter; $k = 1$ proves that translational diffusion of αBc follows HS behavior on the basis of the steric volume fraction, indicating only rather weak inter-protein interactions.

(De)coupling of Rotational Diffusion from Long-Time Translation and Macro-viscosity Is Protein Specific. For the three proteins investigated, the NMR and FCS results for the apparent rotational tumbling times $\tau_{\mathrm{r,ini}}$ are now compared to translational diffusion and the macro-viscosity; see again Figure 5. Notably, the (de)coupling of rotational diffusion from translational diffusion and viscosity is evidently protein specific. Such behavior is in line with an increased importance of protein-specific intermolecular interactions and shape effects for rotational dynamics.[18,46,47] Note that, in our experiments, rotation is never observed to be more retarded than translation.

Both fluorescence spectroscopy data[20] and computer simulations[47] have revealed a decoupling between translational and rotational diffusion that is in full accordance with the αBc results.[22] In contrast, an NMR study of hetero-crowding[21] reported a decoupling in the opposite sense, i.e., rotational diffusion becoming more retarded than translational diffusion and viscosity. Colloid theories[24,25] suggest that rotation in concentrated solutions is expected either to be less affected than or to scale with translation, provided that the concentration of dispersed colloids is well below the onset of the colloidal glass transition. Likely, the unexpected finding of ref 21 results from estimating rotational correlation times solely from site-resolved NMR T_1/T_2 ratios[48] at a single resonance frequency, neglecting the non-exponential nature of the TCF. As has been shown recently,[32] such a treatment can lead to an erroneous estimation of the tumbling correlation time, especially at high concentrations. Systematic deviations are, however, hardly detectable by the traditional approach.[32]

Coupling or decoupling of rotational from long-time translational diffusion and the relationship of these two quantities to the macroscopic viscosity can be generally assigned to the presence or absence of correlated motions among neighboring particles. For long-time diffusion, multiple independent encounters with other particles, that may have to rearrange cooperatively at high concentrations,[13] lead to its dependence on an average friction corresponding to the macroscopic zero-shear viscosity $\eta(\phi)$. In contrast, on the time scale of rotational diffusion (0.01−0.1 μs for HEWL, and ∼1 μs for αBc) the protein's local surrounding neither undergoes substantial reconfiguration, nor do particle collisions appreciably affect the rotational dynamics. In the absence of specific interactions rotational diffusion is almost unhindered.[38] Specifically, even a non-spherical object such as HEWL subject to *only* excluded-volume effects was shown to be able to rotate rather freely within its cage formed by the surrounding particles.[38] Still, local hydrodynamic effects[33] mediated via particle−solvent interactions retard rotational diffusion and account for a measurable but rather weak concentration dependence. In fact, we find that the slow-down of rotational diffusion of αBc with increasing concentration is again quantitatively reproduced by applying a corresponding HS model,[18,49]

$$\frac{\tau_{\mathrm{r}}(\phi_{\mathrm{HS}})}{\tau_{\mathrm{r},0}} \cong [1-0.631\phi_{\mathrm{HS}}-0.762{\phi_{\mathrm{HS}}}^2]^{-1} \quad (6)$$

without requiring rescaling of the effective HS volume fraction ($k = 1$, as for translational diffusion); see Figure 5. Thus, the viscosity experienced by rotation is closer to that of the solvent than to the macroscopic viscosity, as often referred to as microviscosity. More precisely, as a short-time quantity rotational diffusion is considered to be sensitive to the viscosity determined in the limit of high shear rates,[18,50] usually denoted as $\eta_\infty(\phi)$. Hence, a decoupling of rotational from long-time translational diffusion is to be expected as long as $\eta_\infty(\phi) \neq \eta(\phi)$, as is well established for spherical colloids.[13,18,24,25] For αBc and, to a lesser extent, BSA, we observe such a behavior.

Rotational vs Short-Time Translational Diffusion. In contrast to translational diffusion measured by PFG NMR, translational diffusion as detected by neutron scattering is measured on short length scales, corresponding to short observation times of 0.3 ns ≤ τ ≤ 5 ns.[33] The corresponding translational root-mean-square displacements amount to about 10 Å or even less, i.e. translational dynamics is probed solely within the cage formed by neighboring molecules. This situation corresponds to the time scale of rotational diffusion. Both rotational and *short-time* translational diffusion are considered, as mentioned above, to be related to $\eta_\infty(\phi)$; hence, one may expect a similar concentration dependence for these two diffusion processes. To address this point, Figure 5 also presents the short-time translational diffusion data for BSA measured by quasielastic neutron backscattering.[33] Indeed, the concentration dependence of short-time translational diffusion coincides with our data on rotational diffusion within the experimental uncertainty. This coincidence also reinforces that NMR relaxometry and FCS provide reliable results regardless of the polydispersity of the protein solution.

Role of Protein−Protein Interactions. HEWL, being a strongly charged protein under our conditions (pD = 3.8, no buffer), behaves qualitatively differently as compared to αBc and BSA; its rotation is fully coupled to long-time translational diffusion and macroscopic viscosity. Here, when using the *same* effective HS volume fraction as for translational diffusion, the hard-sphere model, eq 6, clearly fails in accounting for the concentration dependence of rotational diffusion (Figure 5). Instead, approaching the experimental data requires a rescaling as large as $k = 3.7$ (compared to $k = 1.5$ for translational diffusion). Moreover, HS modeling intrinsically predicts a

DOI: 10.1021/jacs.6b06615
J. Am. Chem. Soc. 2016, 138, 10365−10372

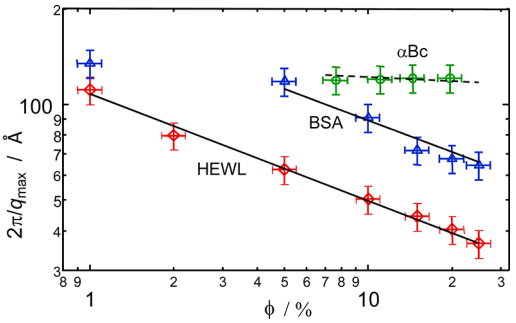

Figure 6. Protein interactions as assessed by SAXS experiments. The plotted inverse maximum positions of the structure factor ($2\pi/q_{max}$) in dependence of the volume fraction ϕ are expected to decrease according to a power law for strong repulsive systems ($q_{max}^{-1} \propto \phi^{-1/3}$, solid lines; BSA at ϕ = 1% was excluded in the fit). The value of $2\pi/q_{max}$ then relates to the average center to center distance between first neighbors. However, in case of screened, hard-sphere-like particles the concentration dependence of $2\pi/q_{max}$ is strongly reduced (the dashed line gives the prediction for spheres with R = 58 Å).

decoupling of rotational from long-time translational diffusion under crowding conditions, see above. Thus, with regard to the same concentration dependence of long-time translational and rotational diffusion, effective-sphere behavior cannot even qualitatively describe the HEWL experimental data. Our finding also stands in stark contrast to results of Brownian dynamics simulations of crowded HEWL solutions when shape effects and only excluded-volume interactions are considered.[38] Consequently, specific interactions must be of major importance and evidently lead to a correlation of the tumbling of a single HEWL molecule with the dynamics of its surroundings.

Our SAXS data (Figure 4) provide direct evidence of the different nature of the interactions present in the three protein solutions studied. A qualitative but easily assessed piece of information is the concentration dependence of the low-q maximum of the structure factor, q_{max} (Figure 6). For a simple HS liquid such as αBc,[29] the maximum of the structure factor does not scale with the mean center-to-center distance of the particles, leading to a constant q_{max}. In contrast, for long-range Coulomb repulsion particles tend to maximize their inter-particle distances. Then, q_{max} can be related to the inverse inter-particle distance by $q_{max} = 2\pi/R_{cc}$ and scales as $\sim\phi^{1/3}$, as is observed for both HEWL and BSA.

Qualitative differences in the charge−charge interactions for our three samples are further documented by the SAXS structure factors (Figure 4). For αBc, again, the HS behavior is supported by the perfect agreement of the experimentally derived structure factor with HS model predictions. In contrast, the structure factor of BSA agrees with the prediction of a screened Coulomb (SC) potential. In case of HEWL, the latter fit still exhibits systematic deviations at small q, indicating the presence of additional short-range attractive forces. This is demonstrated by comparison of the experimentally derived structure factor with the structure factor prediction of a SC potential and a SC potential with an additional short-range attractive Yukawa potential. The obtained ranges of about 39 and 2 Å for the long-range repulsive and short-range attractive interactions, respectively, are consistent with literature[51,52] and match the behavior of patchy charged colloids.[53,54]

The different nature of intermolecular interactions in αBc, BSA, and HEWL solutions is also corroborated by the small but significant differences in the temperature dependence of viscosity and long-time translational diffusion shown in Figure 2. The remarkable non-Arrhenius behavior and the somewhat increased (apparent) activation energy of HEWL at low temperatures as compared to that of pure water reflects significant inter-protein interactions and correlated motions, which ultimately lead to a calorimetric glass transition at high concentrations.

As a result of the short-range attraction, HEWL has long been discussed to form transient clusters upon increasing the concentration.[55,56] The fact that attractive interactions are known to retard rotational diffusion beyond the limit of HS behavior[57] suggests that the phenomena may have a common origin. Note, however, that at all HEWL concentrations, our data on long-time translational diffusion (ms time scale) agree with the diffusion of monomers, which is not found in systems characterized by transient clustering.[37] Further work is certainly necessary to explore this issue.

Since the high overall charge of the HEWL monomers leads to repulsion, this in turn leading to decoupling rather than coupling of rotation and macro-viscosity in the case of isotropic spheres,[57] we suggest that the behavior of HEWL may be related to either a non-uniform charge distribution or charge-enhanced hydrodynamic effects combined with shape anisotropy, to be discussed below. Note that electrostatic multipole interactions and alignment effects give rise to net attractive interactions,[53] providing a rationale for the short-range attraction discussed above.

The quantitative understanding of anisotropic interactions between "patchy" charged colloids as a suitable model for proteins is of substantial current interest,[58] yet recent reports only focus on static structural and thermodynamic properties,[53,54,59] in particular protein solution-phase behavior.[60−63] We are so far not aware of any theoretical assessment of tumbling motion in such cases. The only experimental observation of rotational−translational coupling in a colloidal system was recently made in a suspension of homogeneously charged platelets.[64] Also in this case, effective-sphere models failed to explain the observation, and it was attributed to electro-hydrodynamic coupling effects.

Additional support of our hypothesis is provided by the increasingly non-exponential, tailed nature of the TCF as detected by NMR relaxometry.[19,32] A similar phenomenon has been described even for spherical colloids at high concentrations,[18,65] where it is most likely due to local concentration fluctuations. As mentioned under Results, a "slow tail" was modeled empirically by a second exponential component with a slower isotropization time τ_s and (small) amplitude a_s. We stress that our previous interpretation of a_s in terms of a "model-free" order parameter S^2_{rot} should be considered critical, in view of the unknown shape of the TCF.[39] More detailed analyses are certainly required to extract physically more meaningful parameters. We just note that the parameter a_s increases with concentration, as expected,[32] and is significantly larger for HEWL than for BSA. The relevance of charge for the apparent "slow tail" was proven by NMR experiments on HEWL solutions at different pH.[19] Along this line, experiments[66] and simulations[67] have demonstrated that HEWL orients along the electric field exerted by another protein (α-lactalbumin, 14 kDa).

In summary, we have discussed evidence that the observed coupling between protein rotational and translational diffusion (and also macroscopic viscosity) may be explained by shape-

DOI: 10.1021/jacs.6b06615
J. Am. Chem. Soc. 2016, 138, 10365−10372

and charge-related anisotropic protein−protein interactions, possibly combined with specific hydrodynamic coupling effects. With this, our results emphasize the importance of a prudent choice of the crowding agent in order to mimic *in vivo* conditions. Macromolecular crowding by flexible, possibly branched random-coil polymers such as Ficoll or polyethylene glycol results in a physically different situation compared to crowding by unevenly charged globular proteins.[11,68,69] At high concentrations, the random coils of flexible-polymer crowders interpenetrate, forming an entangled medium that is better described by established polymer physics concepts rather than colloid concepts based on excluded volume only.[68]

CONCLUSIONS

Upon increasing the concentration of globular proteins of widely different size and interactions, PFG NMR and FCS results on translational diffusion measured on a millisecond time scale are consistent and exhibit a scaling with the macroviscosity. Such behavior confirms the wide applicability of the generalized Stokes−Einstein relation for both mono- and polydisperse protein solutions.

In contrast, rotational diffusion, as assessed complementarily by NMR relaxometry and polarized FCS, is a short-time quantity, which is sensitive to the viscosity of the microenvironment. In case of weakly interacting, near-isotropic particles it is close to the viscosity of pure solvent, with only small corrections due to local hydrodynamics. However, a nonspherical shape and/or specific anisotropic interactions lead to a correlation between the rotations of neighboring proteins, coupling the tumbling motion to the macroscopic zero-shear viscosity.

We have found that the applicability of either scenario is protein-specific and that the whole range between these limiting cases known in colloid science is covered: our results reflect both full coupling and strong decoupling between rotational and translational diffusion (HEWL and αBc, respectively), as well as an intermediate case (BSA). SAXS measurements reflecting inter-particle interactions and previous NMR data[19,32] emphasize the relevance of charge effects, combined with hydrodynamic coupling and transient anisotropy arising from a complex surface charge distribution and/or a non-spherical shape. This view is supported by patchy charge models that emphasize the relevance of mutual alignment effects.[53,54,70]

Theoretical assessments of the tumbling motion of concentrated patchy charged colloids and especially proteins are so far not available, but we hope that our work provides a stimulus to develop a more complete physical understanding. This is also important for future NMR studies, in particular of crowded proteins, where the non-exponential character of the tumbling correlation function (TCF) with its apparent "slow tail", which likely arises from anisotropic protein−protein interactions, challenges established data analysis models.[32] Precise knowledge of the TCF may enable the development of physically well motivated and thus precise approaches.[39,40,71] Such endeavors will likely benefit from the complementarity of NMR and FCS results presented herein.

ASSOCIATED CONTENT

Supporting Information

The Supporting Information is available free of charge on the ACS Publications website at DOI: 10.1021/jacs.6b06615.

PFG NMR and sub-ensemble effects (SI1); polarized FCS (SI2); X-ray scattering experiments (SI3); polydispersity and anisotropy effects in NMR relaxometry (SI4); size polydispersity effect on rotational diffusion of αBc (SI5); absolute values of NMR-based translational and rotational diffusion coefficients, and extrapolation to zero concentration (SI6); volume fractions and inter-particle distances (SI7) (PDF)

AUTHOR INFORMATION

Corresponding Authors

*krushelnitsky@physik.uni-halle.de

*kay.saalwaechter@physik.uni-halle.de

Author Contributions

§M.R. and M.O. contributed equally.

Notes

The authors declare no competing financial interest.

ACKNOWLEDGMENTS

We thank T. Thurn-Albrecht (Martin Luther Universität Halle-Wittenberg) for providing access to the SAXS equipment and for helpful discussions. The authors are indebted to the Deutsche Forschungsgemeinschaft (DFG, SFB-TRR 102 project A08) for funding this work.

REFERENCES

(1) Zimmerman, S. B.; Trach, S. O. *J. Mol. Biol.* **1991**, *222*, 599.
(2) Medalia, O.; Weber, I.; Frangakis, A. S.; Nicastro, D.; Gerisch, G.; Baumeister, W. *Science* **2002**, *298*, 1209.
(3) Ellis, R. J. *Trends Biochem. Sci.* **2001**, *26*, 597.
(4) Ellis, R. J. *Curr. Opin. Struct. Biol.* **2001**, *11*, 114.
(5) Ellis, R. J.; Minton, A. P. *Nature* **2003**, *425*, 27.
(6) Zhou, H. X.; Rivas, G. N.; Minton, A. P. *Annu. Rev. Biophys.* **2008**, *37*, 375.
(7) Klumpp, S.; Scott, M.; Pedersen, S.; Hwa, T. *Proc. Natl. Acad. Sci. U. S. A.* **2013**, *110*, 16754.
(8) Cheung, M. S.; Klimov, D.; Thirumalai, D. *Proc. Natl. Acad. Sci. U. S. A.* **2005**, *102*, 4753.
(9) Miklos, A. C.; Sarkar, M.; Wang, Y.; Pielak, G. J. *J. Am. Chem. Soc.* **2011**, *133*, 7116.
(10) Senske, M.; Törk, L.; Born, B.; Havenith, M.; Herrmann, C.; Ebbinghaus, S. *J. Am. Chem. Soc.* **2014**, *136*, 9036.
(11) Danielsson, J.; Mu, X.; Lang, L.; Wang, H.; Binolfi, A.; Theillet, F.-X.; Bekei, B.; Logan, D. T.; Selenko, P.; Wennerström, H.; Oliveberg, M. *Proc. Natl. Acad. Sci. U. S. A.* **2015**, *112*, 12402.
(12) Ando, T.; Skolnick, J. *Proc. Natl. Acad. Sci. U. S. A.* **2010**, *107*, 18457.
(13) Koenderink, G. H.; Philipse, A. P. *Langmuir* **2000**, *16*, 5631.
(14) Segre, P. N.; Meeker, S. P.; Pusey, P. N.; Poon, W. C. K. *Phys. Rev. Lett.* **1995**, *75*, 958.
(15) Banchio, A. J.; Nägele, G.; Bergenholtz, J. *J. Chem. Phys.* **1999**, *111*, 8721.
(16) Banchio, A. J.; Bergenholtz, J.; Nägele, G. *Phys. Rev. Lett.* **1999**, *82*, 1792.
(17) Gupta, S.; Stellbrink, J.; Zaccarelli, E.; Likos, C. N.; Camargo, M.; Holmqvist, P.; Allgaier, J.; Willner, L.; Richter, D. *Phys. Rev. Lett.* **2015**, *115*, 128302.
(18) Koenderink, G. H.; Zhang, H.; Aarts, D. G. A. L.; Lettinga, M. P.; Philipse, A. P.; Nägele, G. *Faraday Discuss.* **2003**, *123*, 335.
(19) Krushelnitsky, A. *Phys. Chem. Chem. Phys.* **2006**, *8*, 2117.
(20) Zorrilla, S.; Hink, M. A.; Visser, A.; Lillo, M. P. *Biophys. Chem.* **2007**, *125*, 298.
(21) Wang, Y.; Li, C.; Pielak, G. J. *J. Am. Chem. Soc.* **2010**, *132*, 9392.
(22) Roos, M.; Link, S.; Balbach, J.; Krushelnitsky, A.; Saalwächter, K. *Biophys. J.* **2015**, *108*, 98.

DOI: 10.1021/jacs.6b06615
J. Am. Chem. Soc. 2016, 138, 10365−10372

(23) Doliwa, B.; Heuer, A. *Phys. Rev. Lett.* **1998**, *80*, 4915.
(24) Kim, M.; Anthony, S. M.; Bae, S. C.; Granick, S. *J. Chem. Phys.* **2011**, *135*, 054905.
(25) Edmond, K. V.; Elsesser, M. T.; Hunter, G. L.; Pine, D. J.; Weeks, E. R. *Proc. Natl. Acad. Sci. U. S. A.* **2012**, *109*, 17891.
(26) Pusey, P. N.; van Megen, W. *Nature* **1986**, *320*, 340−342.
(27) Pusey, P. N.; van Megen, W. *Phys. Rev. Lett.* **1987**, *59*, 2083.
(28) Pusey, P. N. *J. Phys.: Condens. Matter* **2008**, *20*, 494202.
(29) Foffi, G.; Savin, G.; Bucciarelli, S.; Dorsaz, N.; Thurston, G. M.; Stradner, A.; Schurtenberger, P. *Proc. Natl. Acad. Sci. U. S. A.* **2014**, *111*, 16748.
(30) Peschek, J.; Braun, N.; Franzmann, T. M.; Georgalis, Y.; Haslbeck, M.; Weinkauf, S.; Buchner, J. *Proc. Natl. Acad. Sci. U. S. A.* **2009**, *106*, 13272.
(31) Licinio, P.; Delaye, M. *J. Colloid Interface Sci.* **1988**, *123*, 105.
(32) Roos, M.; Hofmann, M.; Link, S.; Ott, M.; Balbach, J.; Rössler, E.; Saalwächter, K.; Krushelnitsky, A. *J. Biomol. NMR* **2015**, *63*, 403.
(33) Roosen-Runge, F.; Hennig, M.; Zhang, F.; Jacobs, R. M. J.; Sztucki, M.; Schober, H.; Seydel, T.; Schreiber, F. *Proc. Natl. Acad. Sci. U. S. A.* **2011**, *108*, 11815.
(34) Bova, M. P.; Ding, L.-L.; Fung, B. K. K.; Horwitz, J. *J. Biol. Chem.* **1997**, *272*, 29511.
(35) Squire, P. G.; Moser, P.; O'Konski, C. T. *Biochemistry* **1968**, *7*, 4261.
(36) Loman, A.; Gregor, I.; Stutz, C.; Mund, M.; Enderlein, J. *Photochem. Photobiol. Sci.* **2010**, *9*, 627.
(37) Rothe, M.; Gruber, T.; Gröger, S.; Balbach, J.; Saalwächter, K.; Roos, M. *Phys. Chem. Chem. Phys.* **2016**, *18*, 18006.
(38) Dlugosz, M.; Antosiewicz, J. M. *J. Chem. Theory Comput.* **2014**, *10*, 481.
(39) Tugarinov, V.; Liang, Z.; Shapiro, Y. E.; Freed, J. H.; Meirovitch, E. *J. Am. Chem. Soc.* **2001**, *123*, 3055.
(40) Meirovitch, E.; Shapiro, Y. E.; Polimeno, A.; Freed, J. H. *J. Phys. Chem. A* **2006**, *110*, 8366.
(41) Finet, S.; Tardieu, A. *J. Cryst. Growth* **2001**, *232*, 40.
(42) Chalikian, T. V.; Totrov, M.; Abagyan, R.; Breslauer, K. J. *J. Mol. Biol.* **1996**, *260*, 588.
(43) Liang, J.; Dill, K. A. *Biophys. J.* **2001**, *81*, 751.
(44) Licinio, P.; Delaye, M. *J. Phys. (Paris)* **1988**, *49*, 975.
(45) van Blaaderen, A.; Peetermans, J.; Maret, G.; Dhont, J. K. G. *J. Chem. Phys.* **1992**, *96*, 4591.
(46) Balbo, J.; Mereghetti, P.; Herten, D.-P.; Wade, R. C. *Biophys. J.* **2013**, *104*, 1576.
(47) Mereghetti, P.; Wade, R. C. *J. Phys. Chem. B* **2012**, *116*, 8523.
(48) Kay, L. E.; Torchia, D. A.; Bax, A. *Biochemistry* **1989**, *28*, 8972.
(49) Cichocki, B.; Ekiel-Jeżewska, M. L.; Wajnryb, E. *J. Chem. Phys.* **1999**, *111*, 3265.
(50) Nägele, G. *J. Phys.: Condens. Matter* **2003**, *15*, S407.
(51) Tardieu, A.; Le Verge, A.; Malfois, M.; et al. *J. Cryst. Growth* **1999**, *196*, 193.
(52) Shukla, A.; Mylonas, E.; Di Cola, E.; Finet, S.; Timmins, P.; Narayanan, T.; Svergun, D. I. *Proc. Natl. Acad. Sci. U. S. A.* **2008**, *105*, 5075.
(53) McClurg, R. B.; Zukoski, C. F. *J. Colloid Interface Sci.* **1998**, *208*, 529.
(54) Yigit, C.; Heyda, J.; Dzubiella, J. *J. Chem. Phys.* **2015**, *143*, 064904.
(55) Porcar, L.; Falus, P.; Chen, W.-R.; Faraone, A.; Fratini, E.; Hong, K.; Baglioni, P.; Liu, Y. *J. Phys. Chem. Lett.* **2010**, *1*, 126.
(56) Cardinaux, F.; Zaccarelli, E.; Stradner, A.; Bucciarelli, S.; Farago, B.; Egelhaaf, S. U.; Sciortino, F.; Schurtenberger, P. *J. Phys. Chem. B* **2011**, *115*, 7227.
(57) Koenderink, G. H.; Lettinga, M. P.; Philipse, A. P. *J. Chem. Phys.* **2002**, *117*, 7751.
(58) Lund, M. *Colloids Surf., B* **2016**, *137*, 17.
(59) Blanco, M. A.; Sahin, E.; Robinson, A. S.; Roberts, C. J. *J. Phys. Chem. B* **2013**, *117*, 16013.
(60) Kern, N.; Frenkel, D. *J. Chem. Phys.* **2003**, *118*, 9882.
(61) Liu, H.; Kumar, S. K.; Sciortino, F. *J. Chem. Phys.* **2007**, *127*, 084902.
(62) Gögelein, C.; Nägele, G.; Tuinier, R.; Gibaud, T.; Stradner, A.; Schurtenberger, P. *J. Chem. Phys.* **2008**, *129*, 085102.
(63) Platten, F.; Valadez-Pérez, N. E.; Castaneda-Priego, R.; Egelhaaf, S. U. *J. Chem. Phys.* **2015**, *142*, 174905.
(64) Kleshchanok, D.; Heinen, M.; Nägele, G.; Holmqvist, P. *Soft Matter* **2012**, *8*, 1584.
(65) Degiorgio, B.; Piazza, R.; Jones, R. B. *Phys. Rev. E: Stat. Phys., Plasmas, Fluids, Relat. Interdiscip. Top.* **1995**, *52*, 2707.
(66) Salvatore, D. B.; Duraffourg, N.; Favier, A.; Persson, B. A.; Lund, M.; Delage, M.-M.; Silvers, R.; Schwalbe, H.; Croguennec, T.; Bouhallab, S.; Forge, V. *Biomacromolecules* **2011**, *12*, 2200.
(67) Kurut, A.; Persson, B. A.; Åkesson, T.; Forsman, J.; Lund, M. *J. Phys. Chem. Lett.* **2012**, *3*, 731.
(68) Soranno, A.; Koenig, I.; Borgia, M. B.; Hofmann, H.; Zosel, F.; Nettels, D.; Schuler, B. *Proc. Natl. Acad. Sci. U. S. A.* **2014**, *111*, 4874.
(69) Holyst, R.; Bielejewska, A.; Szymanski, J.; Wilk, A.; Patkowski, A.; Gapinski, J.; Zywocinski, A.; Kalwarczyk, T.; Kalwarczyk, E.; Tabaka, M.; Ziebacz, N.; Wieczorek, S. A. *Phys. Chem. Chem. Phys.* **2009**, *11*, 9025.
(70) Grant, M. L. *J. Phys. Chem. B* **2001**, *105*, 2858.
(71) Meirovitch, E.; Shapiro, Y. E.; Polimeno, A.; Freed, J. H. *Prog. Nucl. Magn. Reson. Spectrosc.* **2010**, *56*, 360.

DOI: 10.1021/jacs.6b06615
J. Am. Chem. Soc. 2016, 138, 10365−10372